

TEMPORAL AND SPATIAL CHANGES OF $\geq 10^{\circ}\text{C}$ ACCUMULATED TEMPERATURE IN HUANG-HUAI-HAI RIVER BASIN, CHINA

YIN, J.¹ – YUAN, Z.^{2*} – YAN, D. H.^{3*} – YANG, Z. Y.³ – WANG, Y. Q.²

¹*Faculty of Resources and Environmental Science, Hubei University, Wuhan 430062, China
(phone: +86-159-2642-1064)*

²*Changjiang River Scientific Research Institute, Changjiang Water Resources Commission of
the Ministry of Water Resources of China, Wuhan 430010, China
(phone: +86-137-1656-5927)*

³*State Key Laboratory of Simulation and Regulation of Water Cycle in River Basin, China
Institute of Water Resources and Hydropower Research, Beijing 100038, China
(phone: +86-135-0103-8825)*

**Corresponding author*

e-mail: yuanzhe_0116@126.com; phone: +86-137-1656-5927

(Received 27th Sep 2019; accepted 4th Feb 2020)

Abstract. Huang-huai-hai River basin is an important grain production area and economic zone of China. Under the impact of global warming, energy resources are changing all around the world. Studying the $\geq 10^{\circ}\text{C}$ accumulated temperature (AT_{10}) is of great importance for the food security and economy of Huang-huai-hai River basin. The slope of AT_{10} and Mann-Kendall statistical test were applied to quantify the trend magnitude and detect the significant trend respectively. And the distribution pattern and movement characteristics had been analysed with GIS technology. The results shown that AT_{10} of Huang-huai-hai River basin has an increasing trend during since 1960s; AT_{10} has a moving tendency towards the northwest and decreased from the southeast region towards the northwest region. The ratio between active area and stable area in different classes has fluctuated during the study period.

Keywords: *Huang-huai-hai River basin, accumulated temperature, spatiotemporal characteristic analysis, global warming*

Introduction

In the long-term interaction process between the climate system and land surface, climatic regionalization and agricultural distribution came into being, which are relatively stable. It has been proven that global mean surface temperature has increased by 0.85°C during 1880-2012. Mean temperature of 2003-2012 has increased by 0.78°C compared to that of 1850-1900 (IPCC, 2013) and the temperature in China also has shown a similar increasing trend (Wang et al., 2013). As a result, climatic zones and plant phenology have responded to these changes. Temperature determines crops' emergence, flowering and maturity dates (Skaugen and Tveito, 2004; Iannucci et al., 2008; Hou et al., 2014), while each plant species has a base temperature above which biological processes are able to function (Major et al., 1983; Stevens et al., 1986; McMaster and Smika, 1988; Hodges et al., 1994; Bonhomme et al., 1994; Olivier and Annandale, 1998; Kadioglu and Saylan, 2001; Berti and Johnson, 2008; Sacks and Kucharik, 2011). Most crops have a base temperature of 10°C known as the active temperature. Previous researches have proven that the change of activity accumulated temperature will affect the growth rate of winter wheat and soybean (Li et al., 2015;

Liang et al., 2015). Lv et al. (2019) has found that when the cumulative temperature was below $3300^{\circ}\text{C}\cdot\text{d}$, the maize yield increased with the cumulative temperature, while when the cumulative temperature was below $3800^{\circ}\text{C}\cdot\text{d}$, the soybean and rice yields increased with the cumulative temperature $\geq 10^{\circ}\text{C}$ accumulated temperature (hereinafter referred to as AT10) is the sum of mean daily temperature during the period in which mean daily temperature is above 10°C for every day (Yan et al., 2011). Accumulated temperature plays a fundamental role in a plant's growth and spatial distribution (Xu et al., 2009). International research on AT10 is limited. Concerning researches on this subject has mainly been focused on the northeast of the China, while very little research has been carried out for Huang-huai-hai river basin (hereinafter referred to as HHHRB).

Using the meteorological data from Mikhelson station, Chirkov and Kononova (1984) analysed the spatial and temporal changes of $\geq 10^{\circ}\text{C}$ AAT in Moscow from 1890 to 1981. Dong et al. (2009) studied the spatiotemporal changes of accumulated temperatures $\geq 10^{\circ}\text{C}$ of China from the late 1980s to 2000 and found out that since the late 1980s it has increased on a national scale. Yan et al. (2011) studied the spatial-temporal changes of various decadal AT10 and the climatic means of $\geq 10^{\circ}\text{C}$ accumulated temperature in the north-eastern China. Significant increase of decadal AT10 since the 1980s was discovered and the change became larger and more obvious in the 1990s and 2000s. Wang et al. (2011) explored the tempo-spatial characteristics of AT10 and the results showed that the AT10 had a decreasing trend from southwest to northeast and also had 2.5-4a oscillations in Northeast China. Wu (2011) studied the changing trend of $\geq 10^{\circ}\text{C}$ accumulated temperature in Shenyang, Liaoning Province of China and found a significant increasing trend. Song et al. (2011) found a significant increase of accumulated temperature and length of growing season of North China Plain from 1961 to 2009. The start of growing season moved up and the end of growing season was delayed.

This paper analysed the spatial and temporal changes of AT10 in HHHRB, China. The tendency, distribution pattern and movement characteristics had been selected for the analysis, which can provide data for the basis of decision making for food security in HHHRB as well as give agriculture production technological support to respond to global warming.

Materials and methods

Study area

Huang-huai-hai River basin (HHHRB) encompasses the Yellow River basin, Huaihe River basin and Haihe River basin. HHHRB is located in the east of China and lies between 32° - 42°N , 110° - 120°E . The entire or partial part of the following provinces form HHHRB: Qinghai Province, Sichuan Province, Gansu Province, Ningxia Hui Autonomous Region, Inner Mongolia Autonomous Region, Shaanxi Province, Shanxi Province, Henan Province, Hebei Province, Shandong Province, Anhui Province, Jiangsu Province, Beijing and Tianjin (*Fig. 1*). The Yellow River basin has an area of $75.2 \times 10^4 \text{ km}^2$. Temperature difference is large and stark regional differences can be seen. The catchment area of Huaihe River basin is $27.5 \times 10^4 \text{ km}^2$ and its temperature increases from the north to the south with the temperature span from 11 to 16°C . For Haihe River basin, it has an area of $31.8 \times 10^4 \text{ km}^2$ and its mean annual temperature ranges from 1.5 to 14°C .

One third of China's population, grain yield and gross domestic product comes from HHRB (Shen et al., 2002; Liu et al., 2010; Yu et al., 2012). As an important grain producing area and economic zone, HHRB plays a fundamental role in guaranteeing China's economic and social development. Thus, studying AT10 in HHRB is of great importance for safeguarding China's food security. In the meantime, data base will be provided for agriculture to response to global warming in the context of climate change.

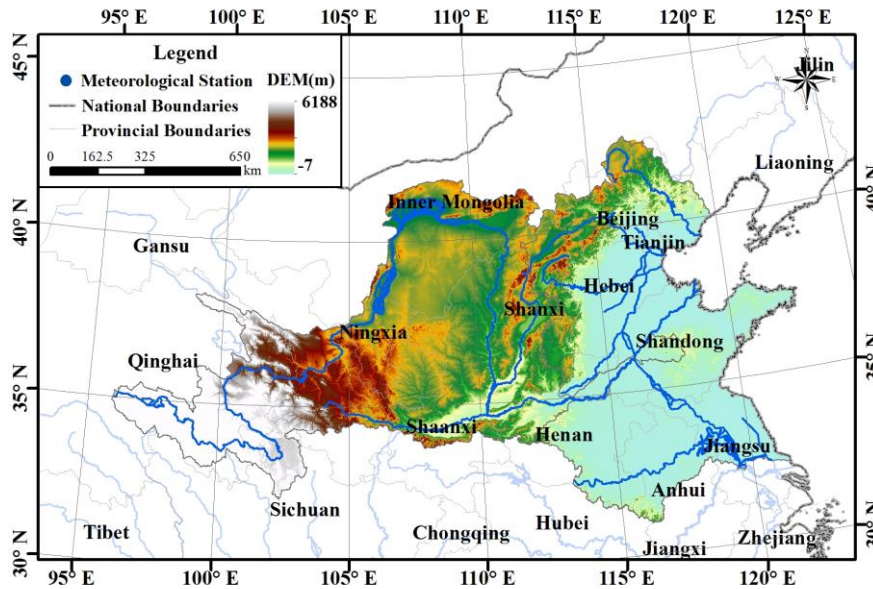


Figure 1. The location of Huang-Huai-Hai River basin

Dataset

The basic data for this study was the time series of daily air temperature, which were obtain from 982 meteorological stations within and surrounding HHRB (Fig. 2). The daily air temperature was download from National Meteorological Information Centre (<http://data.cma.cn/>). Inverse Distance Weighted (IDW) spatial interpolation was used to create daily grid data (5 km \times 5 km) of temperature. Data processing process was based on ArcInfo Workstation 10.0 platform using the ARC Macro Language (AML) to conduct the relevant calculations.

Methodology

Calculation of $\geq 10^{\circ}\text{C}$ accumulated temperature

The AT10 in each grid were calculated with 5-day simple moving average temperature in this study, which is defined as Equation 1.

$$AT10_n = \sum_{i=1}^D T_i \quad (\text{Eq.1})$$

$$T_i = \begin{cases} Ta_i & Ta_i \geq 10 \\ 0 & Ta_i < 10 \end{cases} \quad (\text{Eq.2})$$

where $AT10_n$ is $\geq 10^{\circ}\text{C}$ accumulated temperature for the n th year. Ta_i is the 5-day simple moving average air temperature for i th day. D is days for the n th year.

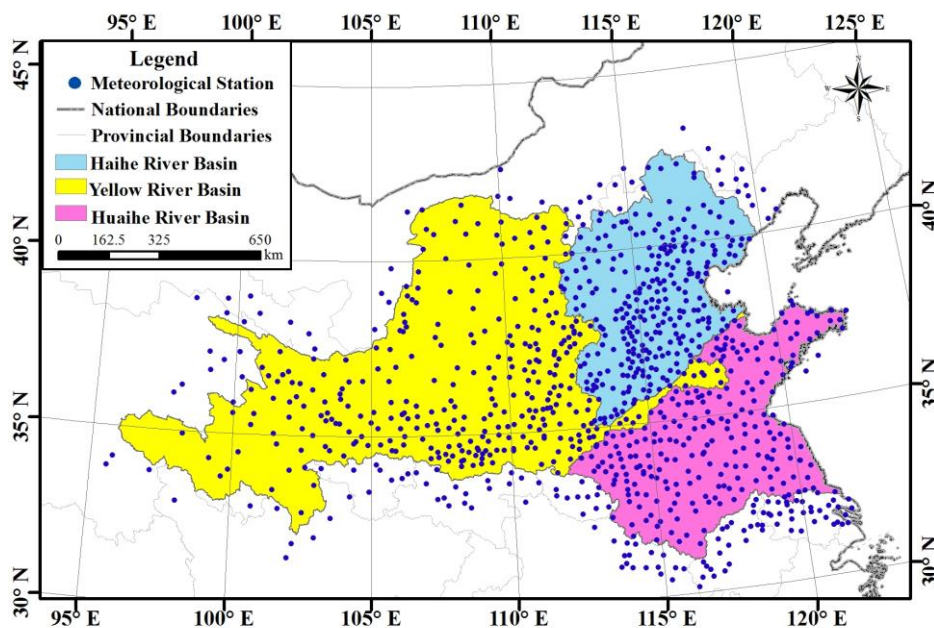


Figure 2. The location of meteorological stations within and surrounding Huang-Huai-Hai River basin

Mann-Kendall trend test

A non-parametric approach, Mann-Kendall statistical test (M-K) (Mann, 1945), is widely used in hydrology and climatology analysis because of less sensitive to outliers than parametric approaches (Hamed, 2009; Tian et al., 2012; Wang et al., 2008). In this study, the M-K method was used to test the tendency of $AT10$ in the HHRB. The test statistic U was established as Equations 3–5.

$$U = \frac{\tau}{\sqrt{V_{ar}(\tau)}} \quad (\text{Eq.3})$$

$$\tau = \frac{4p}{n(n-1)} - 1 \quad (\text{Eq.4})$$

$$V_{ar(\tau)} = \frac{2(2n+5)}{9n(n-1)} \quad (\text{Eq.5})$$

where n is the length of the data sequence and p is the allelomorph of the random sequence. If U is positive the sequence has an increasing trend, if U is negative the sequence has a decreasing trend, and if $|U| > U\alpha = 1.96$ while the significance level is $\alpha = 0.05$, then the sequence has passed the significance test with a significant changing trend.

Linear regression analysis and the slope

Linear regression method was utilized to calculate the slope of annual mean AT10 of HHHRB. Its tendency was analyzed and a test for significance was done (Zhang et al., 2011).

$$\text{Slope} = \frac{n \times \sum_{i=1}^n (i \times K_i) - \sum_{i=1}^n i \sum_{i=1}^n K_i}{n \times \sum_{i=1}^n i^2 - (\sum_{i=1}^n i)^2} \quad (\text{Eq.6})$$

where slope is the tendency rate, n is the number of whole study years, and K_i is the AT10 in the i th year. If $\text{slope} > 0$ in a certain area, it means that the AT10 in this area has an increasing trend from 1956-2011.

Geographic center for $\geq 10^{\circ}\text{C}$ accumulated temperature

On the platform of ARCGIS10.0, the ARC Macro Language (AML) was used to conduct the analysis. For each different class of AT10 of HHHRB, CENTROIDLABLES was utilized to calculate the longitude and latitude of each continuous partition's centroid (x_i, y_i). After that, area was used as the weight to compute the centroid of each class of AT10 of HHHRB:

$$X_a = \frac{\sum_{i=1}^n x_i s_i}{\sum_{i=1}^n s_i} \quad (\text{Eq.6})$$

$$Y_a = \frac{\sum_{i=1}^n y_i s_i}{\sum_{i=1}^n s_i} \quad (\text{Eq.7})$$

where, x_a is the longitude of the centroid for a certain class of AT10 of HHHRB, x is the longitude of the centroid of each partition, s is the area of each partition, and n is the number of partitions in a certain class of AT10 of HHHRB. The calculation method for latitude is the same as that for longitude.

Results and analyses

Temporal changes of $\geq 10^{\circ}\text{C}$ accumulated temperature in HHHRB

The maximum value, minimum value, range (difference between maximum value and minimum value) and standard deviation of AT10 temperature of HHHRB were calculated (Fig. 3). The test statistic values for maximum value, minimum value, range and standard deviation of AT10 were 5.203, 3.223, 4.976 and 4.947, respectively. It could be concluded that all the characteristic values had a significant increasing trend at the 95% confidence level.

Annual accumulated temperature is an important factor which will affect the crop yield. The grain yield per hectare has a positive correlation with accumulated

temperature (Wang et al., 2011). The range of AT10 of HHHRB increased while the maximum value and minimum value both increased as well which is consistent with the trend of global warming. What was also revealed was that since 1956, energy resources in the study area has increased, which will help to produce more food (Anwar et al., 2013). However, the risk of drought will be increased at the same time.

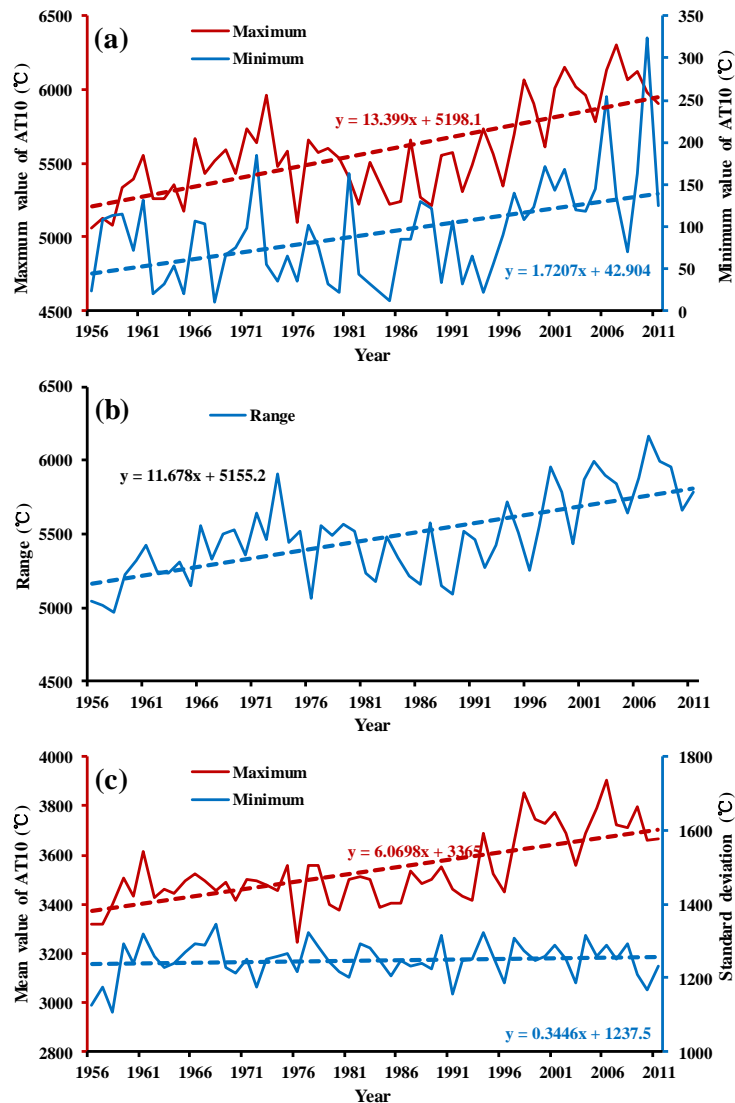


Figure 3. Maximum/minimum value (a), range (b) and standard deviation (c) of AT10 of HHHRB

Another factor which has great impact on crop growth is the length of thermal growing season. In this study the duration of development period, time started and ending time of AT10 were calculated for the HHHRB (Fig. 4). Since 1956, duration of thermal growing season of AT10 of HHHRB has an increasing trend. $U_{\text{duration}} = 4.142$ which has passed the significance test at the 95% level. The starting time of thermal growing season has moved forward with $U_{\text{time started-min}} = -1.145$, but it has not passed the significance test at the 95% level. The ending time has been postponed with $U_{\text{ended time-max}} = 0.297$, but it still has not passed the significance test at the 95% level.

This result shows that the length of the thermal growing season of HHHRB from 1956-2011 has extended and may be a potential outcome of global warming in the river basin. The start of the growing season has moved forward while the end of growing season has lagged. To examine the effect of temporal changes in AT10 the whole study period (1956-2011) is be divided into 7 phases for each decade: A for 1956-1959, B for 1960-1969, C for 1970-1979, D for 1980-1989, E for 1990-1999, F for 2000-2009 and G for 2010-2011. Duration of thermal growing season of $\geq 10^{\circ}\text{C}$ accumulated temperature of HHHRB in each phase was calculated, which are 209.5 days, 214.3 days, 210.4 days, 212.0 days 218.1 days, 222.6 days and 225.2 days. Compared with that of phase A, the duration of F and G have increased significantly by 13.1 days and 15.7 days, respectively. The thermal conditions of HHHRB have improved for crop growth during 1956-2011, thus crop production may benefit from this increasing trend.

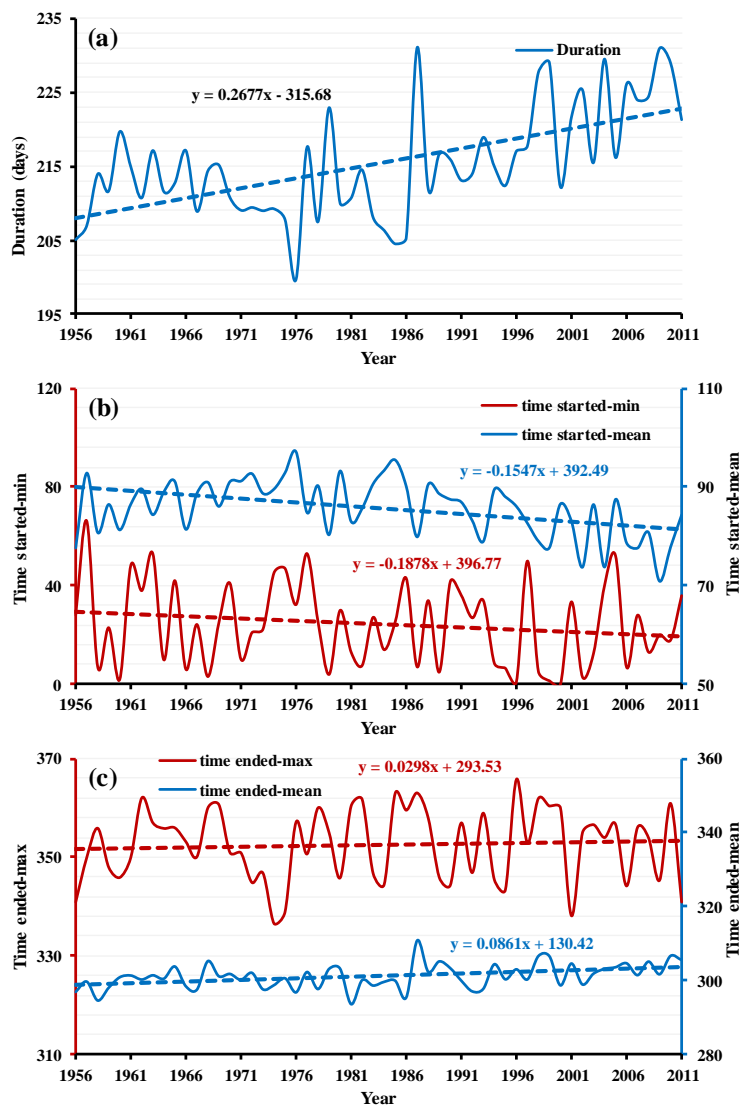


Figure 4. Duration (a), time started (b) and ended time (c) of thermal growing season of AT10 of HHHRB. (Time started-min is the minimum value of the start time of all the grids in the study area, time started-mean is the mean value of the start time of all the grids in the study area, ending time-max is the maximum value of the ending time of all the grids in the study area, and ending time-mean is the mean value of the ending time of all the grids in the study area)

Spatial changes of $\geq 10^\circ\text{C}$ accumulated temperature of HHHRB

Distribution pattern of $\geq 10^\circ\text{C}$ accumulated temperature of HHHRB

Temperature belts are defined into 5 classes for AT10 to study its spatial distribution as follows: (1) Cold temperature zone where the AT10 is less than 1600°C . The planting system is one crop a year and its main crops are early-matured spring wheat, barley, potato, etc. (2) Mid temperate zone where the AT10 is less than 3400°C while more than 1600°C . The planting system is one crop a year and its main crops are spring wheat, soybean, maize, millet, sorghum, etc. (3) Warm temperate zone where the AT10 is less than 4500°C while more than 3400°C . The planting system is three crops every two years or two crops a year consisting mainly of multiple cropping buckwheat after winter wheat or multiple cropping maize, millet and sweet potato after winter wheat, etc. (4) Subtropical zone where the AT10 is less than 8000°C while more than 4500°C . The planting system is two or three crops a year. The rotation system is wheat-rice rotation or double-rice rotation, etc. (5) Where the AT10 is more than 8000°C , the planting system is three crops a year and its main crops are rice, sugarcane, etc.

According to the classification standard mentioned above, decadal spatial distribution patterns of AT10 of HHHRB from 1956-2011 were analysed. Since the AT10 of the whole study area is less than 8000°C , only (1), (2), (3) and (4) were analysed. Generally speaking, AT10 of HHHRB decreased from southeast to northwest (Fig. 5). Distribution area of AT10 of different classes were calculated as well as the tendency of the distribution area: $U_{(1)} = -5.527$, $U_{(2)} = -4.919$, $U_{(3)} = 2.375$, $U_{(4)} = 4.227$. Distribution area of class (1) and (2) have a downward trend while that of class (3) and (4) have an upward trend. All of them have passed the significance test at 95% level (Fig. 6).

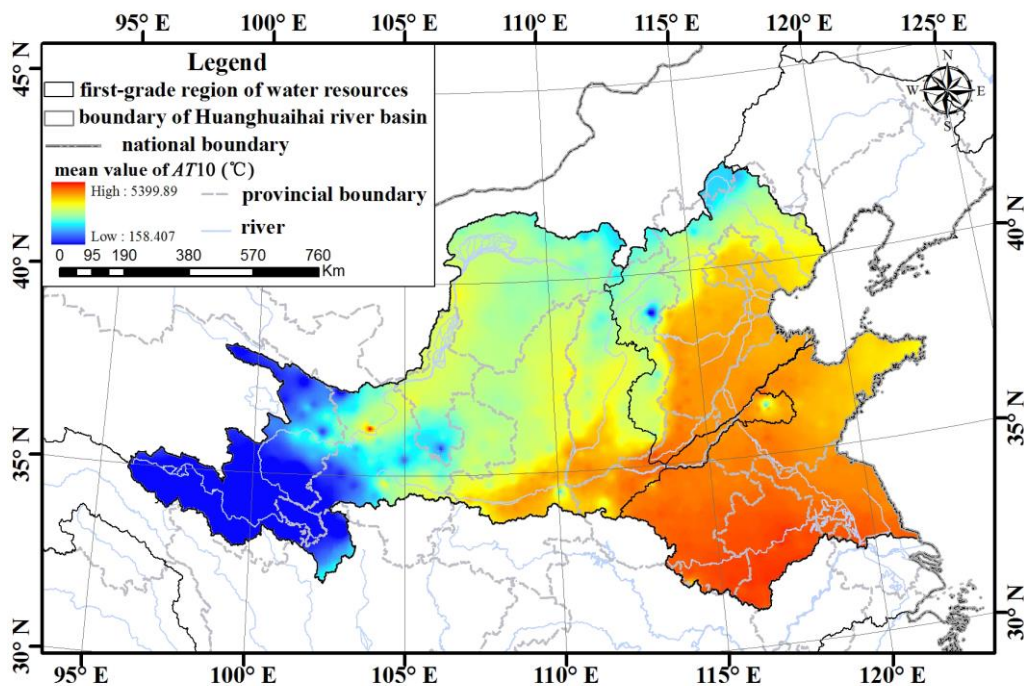


Figure 5. Spatial distribution of AT10 of HHHRB

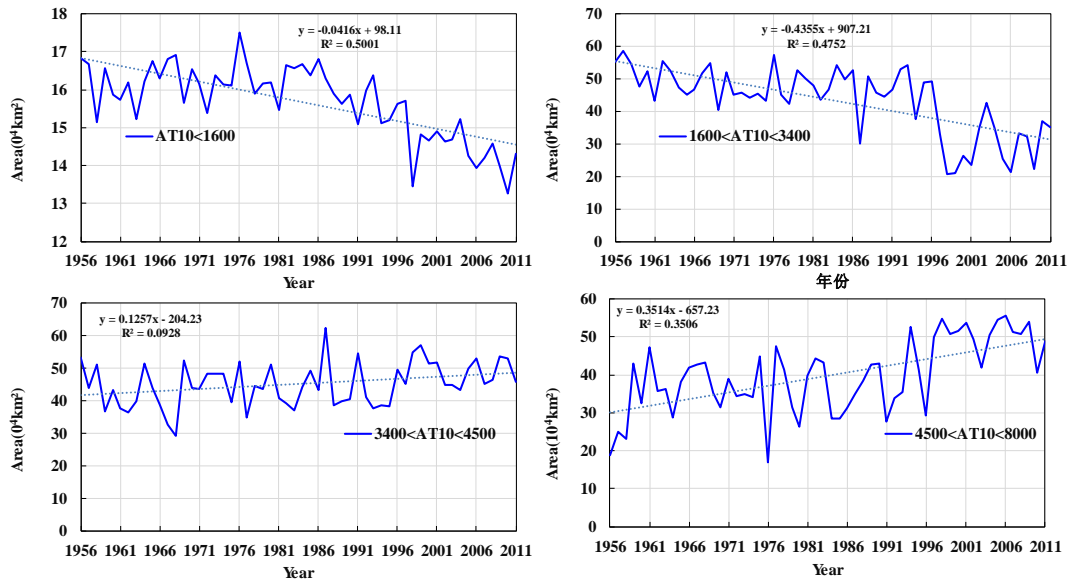


Figure 6. Area of different classes of AT10 of HHHRB

For each grid of a certain class of AT10 of HHHRB, the accumulated temperature either fits in the class or does not. By dividing the number of years when the accumulated temperature fits in a given class by the total number of years of the study period, the frequency of the occurrence of AT10 in a certain class in each grid can be obtained. The spatial distribution of the frequency of AT10 in HHHRB for each class are displayed in (Fig. 7).

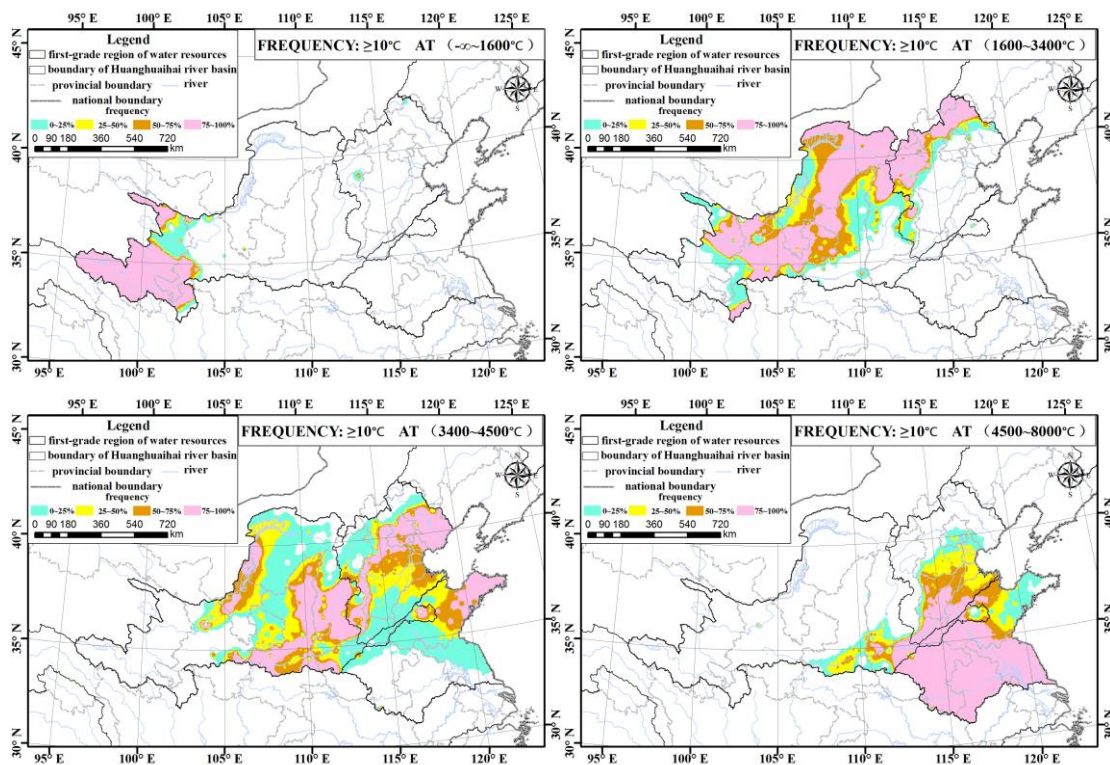


Figure 7. Spatial distribution of the frequency of AT10 of HHHRB in different classes

Most of the regions in class (1) consist of high frequencies except in the northeast region. For class (2), the region of highest frequency lies mainly in the central region, while the periphery is the low frequency region. In addition, the area of high frequency region is significantly larger than the area of low frequency region. For class (3), the high frequency region lies in the middle and the low frequency region lies on its two sides. The area of high and low frequency regions is approximately the same. For class (4), most of its area is high frequency region, while the northwest rim is in the low frequency region.

From *Figures 8 and 9* we could see that except the most westerly part and some scattered areas, AT10 of HHHRB has an increasing trend. Additionally, the trend in most areas has passed the significance test at the level of 95%.

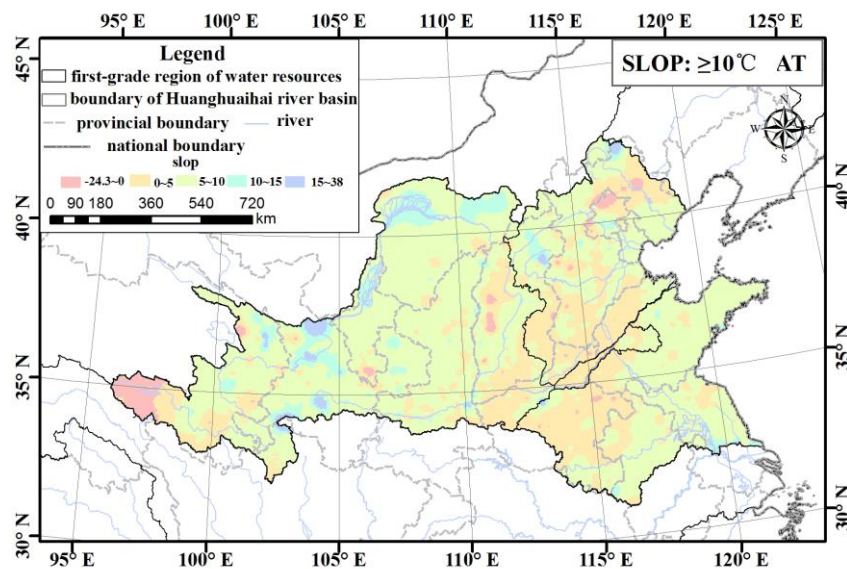


Figure 8. Slope of AT10 of HHHRB

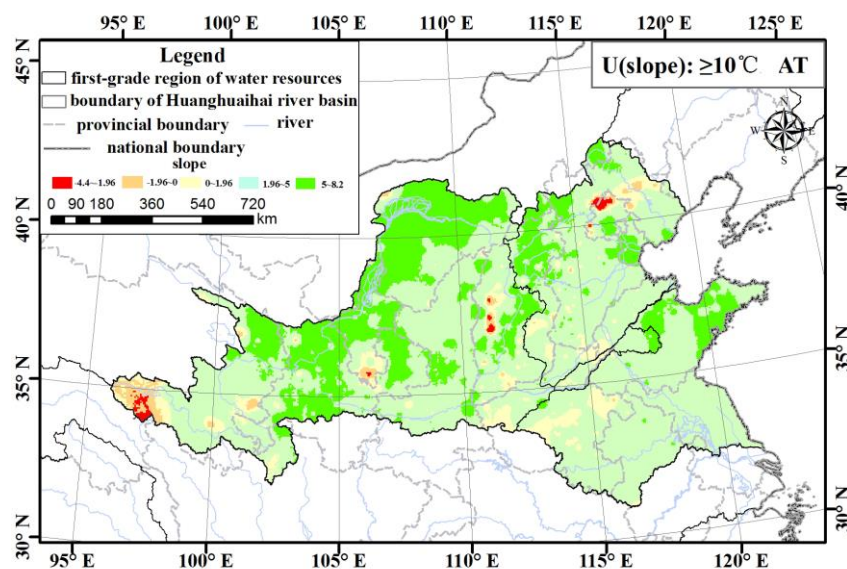


Figure 9. U value of the slope of AT10 of HHHRB

Movement characteristics of $\geq 10^{\circ}\text{C}$ accumulated temperature of HHHRB

From Figure 10 we can see that class (1) of AT10 of HHHRB has a moving tendency towards southwest. $U_{(1)\text{longitude}} = -5.710$ and $U_{(1)\text{latitude}} = -6.742$. They both have passed the significance test at 95% level. For class (2), $U_{(2)\text{longitude}} = -2.572$ so the westward trend of class (2) is significant. $U_{(2)\text{latitude}} = -1.697$, therefore class (2) has a southward trend but is not significant. For class (3), $U_{(3)\text{longitude}} = -5.612$ and $U_{(3)\text{latitude}} = 3.703$, thus class (3) has a significant trend moving towards northwest. For class (4), $U_{(4)\text{longitude}} = -1.682$ and $U_{(4)\text{latitude}} = 4.311$. So the northward trend is significant while the westward trend is not significant.

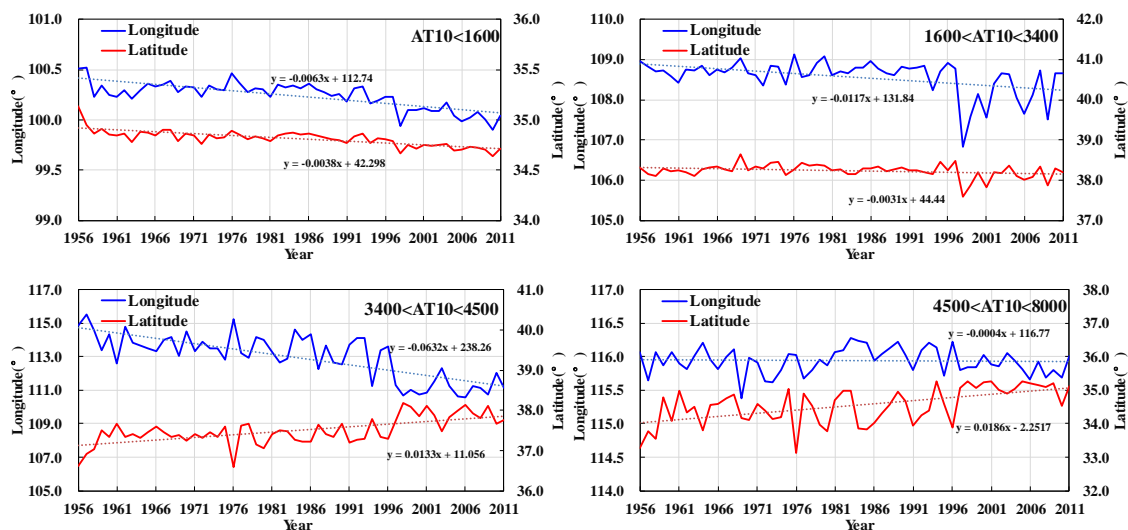


Figure 10. Movement characteristics of AT10 of HHHRB

The study period 1956-2011 was divided into 7 phases: A-G. Since phase A only includes four years, which are 1956, 1957, 1958 and 1959, and phase G only includes 2010 and 2011, phase A and G were deleted in the following analysis. For the remaining phases, spatial distribution of active area and stable area of the study area of AT10 were analysed (Fig. 11; Table 1). In a given phase, active area is the area where a certain class of AT10 appeared one or more times. Stable area is the area where the occurrence number of a certain class of AT10 is equal to the number of study years in a given phase.

For class (1), decadal change of active area and stable area are not obvious. For class (2), both stable area and active area are moving towards northwest and their areas are decreasing. For class (3), stable area and active area also have a moving trend towards northwest, which is particularly obvious in 2000-2010. For class (4), active area did not change much, while stable area moved northward notably during 2000-2010.

For class (1), the ratio between active and stable areas has been around 1:9. For class (2), the ratio between active and stable areas has changed from 4:6 to 6:4, thus the ratio of active area has increased. For class (3), the ratio between active and stable areas has changed from 7:3 to 6:4, thus the ratio of active has decreased. For class (4), the ratio between active and stable areas has changed from 4:6 to 5:5, and then back to 3:7, thus the ratio between these two areas have reversed.

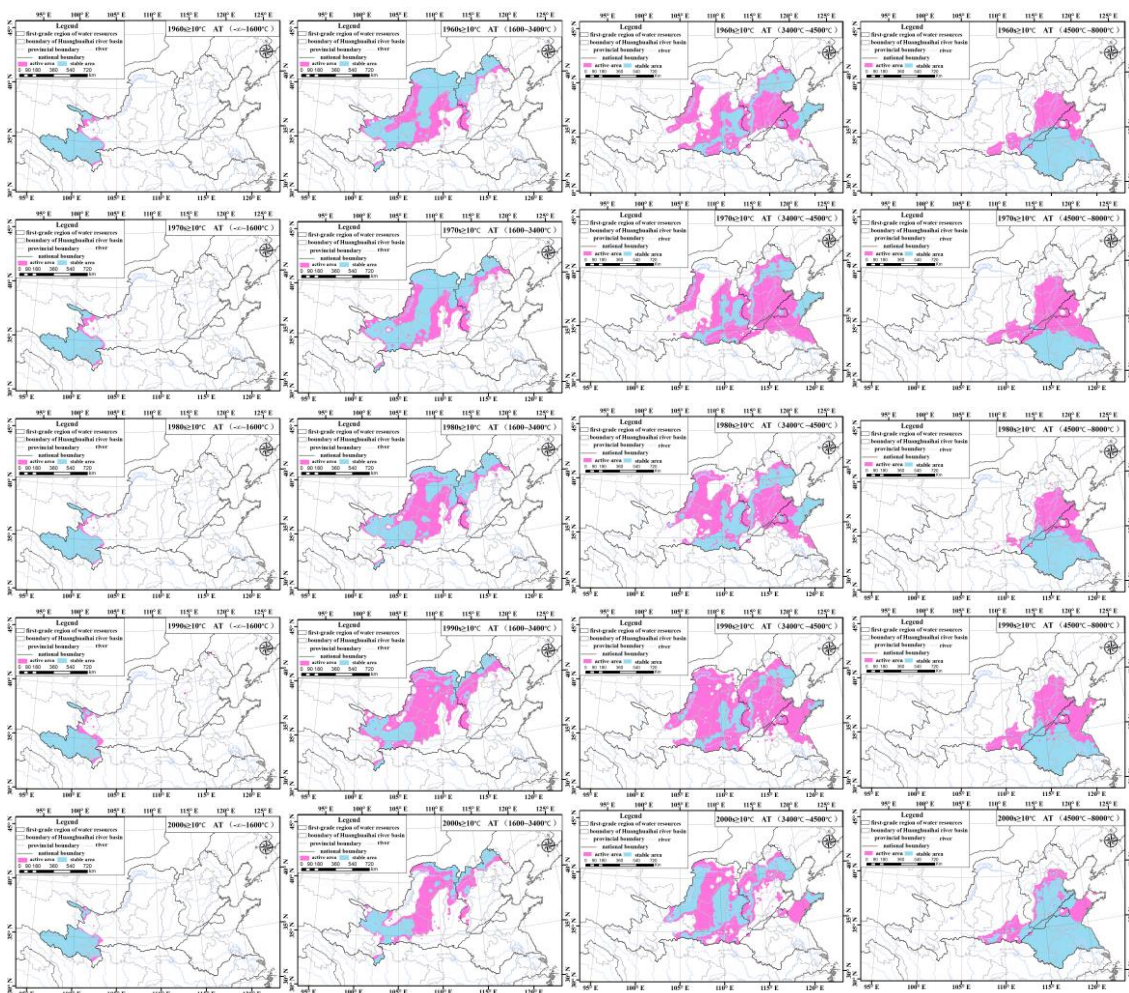


Figure 11. Decadal spatial movement characteristics of active area and stable area of different classes of $\geq 10^{\circ}\text{C}$ ATT of HHHRB

Conclusion and discussion

In general, AT_{10} of HHHRB has an increasing trend during the study period, which is in accordance with the paradigm of global warming. Since 1956, energy resources in the HHHRB have increased. On one hand, this will contribute to the food production in the study area but on the other, the risk of drought could be increased. The maximum value, minimum value, range and standard deviation of AT_{10} of HHHRB all had a significant increasing trend, which verified significant warming and increasing energy resources in the study area. Duration of thermal growing season of AT_{10} of HHHRB has an increasing trend. The starting time of thermal growing season has moved up and the ending time has been postponed. Compared with the duration of phase A, the duration of F and G have increased significantly by 13.1 days and 15.7 days respectively.

Generally speaking, AT_{10} of HHHRB has a moving tendency towards the northwest. AT_{10} of HHHRB decreased from the southeast region towards the northwest region. Except the west most part and some scattered area, AT_{10} of HHHRB has a significant increasing trend. Area of class (1) and (2) have a downward trend while that of class (3) and (4) have an upward trend. Class (1), (2), (3) and (4) of AT_{10} of HHHRB have a

moving tendency towards southeast, west, northwest and north respectively. For class (2) and (3), stable area and active area are moving towards the northwest. The active area and stable area of class (1) have not experienced a notable change. For class (4), stable area moved northward but the active area remained changeless. What is more, the ratio between active area and stable area in different classes has fluctuated during the study period.

Table 1. Decade ratio of active area and stable area of different classes of AT10 of HHHRB (100%)

Class	(1)				
	1960s	1970s	1980s	1990	2000s
Active area	11.9	13.7	9.9	18.1	9.2
Stable area	88.1	86.3	90.1	81.9	90.8
Class	(2)				
	1960s	1970s	1980s	1990	2000s
Active area	40.2	39.5	50.5	69.9	58.3
Stable area	59.8	60.5	49.5	30.1	41.7
Class	(3)				
	1960s	1970s	1980s	1990	2000s
Active area	67.3	74.1	65.1	80.3	56.9
Stable area	32.7	25.9	34.9	19.7	43.1
Class	(4)				
	1960s	1970s	1980s	1990	2000s
Active area	43.4	66.0	45.2	54.5	27.2
Stable area	56.6	34.0	54.8	45.5	72.8

Ratio of active area in a certain phase and a certain class = (area of active area) / (area of active area + area of stable area); ratio of stable area in a certain phase and a certain class = (area of stable area) / (area of active area + area of stable area)

In the previous studies, Zhao et al. (2016) have found that the accumulated temperature had a strong positive effect on the components of maize yield in East Gansu. Wang et al. (2006) have detected that winter wheat yield increased with the increase of AT10, but decreased with the increase of AT20. The climate change would affect the crop productivity and food supply, which decrease the stability of the global food system. However, the potential impact on a regional scale is unclear (Wheeler et al., 2013). Global Climate change and regional climate change are not completely consistent due to the large regional differences in natural environment and human behavior. It is necessary to analyze the characteristics of regional accumulated temperature and its impact on local crop yield in the context of global climate change.

Acknowledgements. This research was funded by [National Key Research and Development Project] grant number [2017YFC1502404]; [National Natural Science Foundation of China] grant number [51909080;51709008]; [the Open Research Fund of State Key Laboratory of Simulation and Regulation of Water Cycle in River Basin (China Institute of Water Resources and Hydropower Research)] grant number [IWHR-SKL-KF201804]; [Young and middle-aged talent project of Hubei Province Education Department] grant number [Q20181001];. Natural Science Foundation of Hubei Province (2018CFB655).

REFERENCES

- [1] Anwar, M. R., Liu, D. L., Macadam, I., Kelly, G. (2013): Adapting agriculture to climate change: a review. – *Theoretical and Applied Climatology* 113: 225-245.
- [2] Berti, M. T., Johnson, B. L. (2008): Physiological changes during seed development of cuphea. – *Field Crops Res* 106: 163-170.
- [3] Bonhomme, R., Derieux, M., Edmeades, G. O. (1994): Flowering of diverse maize cultivars in relation to temperature and photoperiod in multi-location field trials. – *Crop Sci* 34: 156-164.
- [4] Chirkov, Y. I., Kononova, N. K. (1984): Inter-annual variations of accumulated temperature from observation data of Mikhelson. – *Meteorology and Hydrology* 11: 102-106.
- [5] Dong, J. W., Liu, J. Y., Tao, F. L., Xu, X. L., Wang, J. B. (2009): Spatio-temporal changes in annual accumulated temperature in China and the effects on cropping systems, 1980s to 2000. – *Climate Research* 40: 37-48.
- [6] Hamed, K. (2009): Exact distribution of the Mann-Kendall trend test statistic for persistent data. – *Journal of Hydrology* 365: 86-94.
- [7] Hodges, D. M., Hamilton, R. I., Charest, C. (1994): A chilling resistance test for inbred maize lines. – *Can. J. Plant Sci* 74: 687-691.
- [8] Hou, P., Liu, Y., Xie, R. Z., Ming, B., Ma, D. L., Li, S. K., Mei, X. R. (2014): Temporal and spatial variation in accumulated temperature requirements of maize. – *Field Crops Research* 158: 55-64.
- [9] Iannucci, A., Terribile, M. R., Martiniello, P. (2008): Effects of temperature and photoperiod on flowering time of forage legumes in a Mediterranean environment. – *Field Crops Res* 106: 156-162.
- [10] IPCC (2013): Summary for Policymakers. – In: Stocker, T. F., Qin, D., Plattner, G.-K., Tignor, M., Allen, S. K., Boschung, J., Nauels, A., Xia, Y., Bex, V., Midgley, P. M. (eds.) *Climate Change 2013: The Physical Science Basis. Contribution of Working Group I to the Fifth Assessment Report of the Intergovernmental Panel on Climate Change*. Cambridge University Press, Cambridge.
- [11] Kadioglu, M., Saylan, L. (2001): Trends of growing degree-days in Turkey. – *Water Air Soil Pollut* 126: 83-96.
- [12] Li, X., Zhang, D., Wang, H., Shao, Y., Ma, F. (2015): Impact of temperature increment before the over-wintering period on growth and development and grain yield of winter wheat. – *Chinese Journal of Applied Ecology* 26(3): 839-846 (in Chinese).
- [13] Liang, Q., Zhang, G., Yin, H. (2015): Effect of Temperature on the growth rate and yield of soybean based on stages seeding. – *Anhui Agricultural Science Bulletin* 21(5): 134-137 (in Chinese).
- [14] Liu, M., Wu, J., Lv, A., Zhao, L., He, B. (2010): The water stress of winter wheat in Huang-Huai-Hai plain of China under rain-fed condition. – *Prog. Geogr.* 29(4): 427-432 (in Chinese).
- [15] Lv, J., Yan, C., Jia, T., Wang, F., Sun, H., Dong, S., Gong, Z. (2019): The variation of accumulated temperature in Songnen Plain and its impact on crop yield. – *Chinese Journal of Ecology* 38(11): 3349-3356 (in Chinese).
- [16] Major, D. J., Brown, D. M., Bootsma, A., Dupuis, G., Fairey, N. A., Grant, E. A., Green, D. G., Hamilton, R. I., Langille, J., Sonmor, G., Smeltzer, G. C., White, R. P. (1983): An evaluation of the corn heat unit system for the short-season growing regions across Canada. – *Can. J. Plant Sci* 63: 121-130.
- [17] Mann, H. B. (1945): Non-parametric test against trend. – *Econometrika* 13: 245-259.
- [18] McMaster, G. S., Smika, D. E. (1988): Estimation and evaluation of winter wheat phenology in the central Great Plains. *Agric. – Forest Meteorol* 43: 1-18.
- [19] Olivier, F. C., Annandale, J. G. (1998): Thermal time requirements for the development of green pea (*Pisum sativum* L.). – *Field Crops Res* 56: 301-307.

- [20] Sacks, W. J., Kucharik, C. J. (2011): Crop management and phenology trends in the U. S. Corn Belt: impacts on yields, evapotranspiration and energy balance. – *Agric. Forest Meteorol* 151: 882-894.
- [21] Shen, F., Geng, L., Qin, F., Xu, P. (2002): Analysis of water saving in received area in Huanghe-Huaihe-Haihe watersheds and Eastern and Middle Lines of water transferring project from South to North, China. – *Adv. Water Sci.* 13(6): 768-774 (in Chinese).
- [22] Skaugen, T. E., Tveito, O. E. (2004): Growing-season and degree-day scenario in Norway for 2021-2050. – *Clim. Res* 26: 221-232.
- [23] Song, Y. L., Zhao, Y. X., and Wang, C. Y. (2011): Changes of accumulated temperature, growing season and precipitation in the North China Plain from 1961 to 2009. – *Acta Meteor. Sinica* 25(4): 534-543.
- [24] Stevens, E. J., Stevens, S. J., Flowerday, A. D., Gardner, C. O., Eskridge, K. M. (1986): Developmental morphology of dent corn and popcorn with respect to growth staging and growth models. – *Agron. J.* 78: 867-874.
- [25] Tian, Y., Xu, Y., Booij, M., Lin, S., Zhang, Q., Lou, Z. (2012): Detection of trends in precipitation extremes in Zhejiang, East China. – *Theoretical and Applied Climatology* 107: 201-210.
- [26] Wang, H., Chen, Y. N., Xun, S., Lai, D. M., Fan, Y. T., Li, Z. (2013): Changes in daily climate extremes in the arid area of northwestern China. – *Theoretical and Applied Climatology* 112(1-2): 15-28.
- [27] Wang, W., Zhang, T., Huang, B., Li, Z., Wang, R., Yang, M., Pu, J. (2006): Responses of winter wheat in the Loess Plateau of east Gansu Province to climate warming. – *Chinese Journal of Ecology* 25(7): 774-778.
- [28] Wang, W., Chen, X., Shi, P., van Gelder, P. H. A. J. M. (2008): Detecting changes in extreme precipitation and extreme streamflow in the Dongjiang River Basin in southern China. – *Hydrology and Earth System Sciences* 12(1): 207-221.
- [29] Wang, Y. H., Ren, C. Y., Han, Y. D., Zhang, J., Zhang, W. Z., Huang, R. D. (2011): The tempo-spatial patterns of active accumulated and consecutive extreme low temperature and their impacts on grain crop yield in Northeast China. – *Journal of Agro-Environment Science* 30(9): 1742-1748.
- [30] Wheeler, T., Von Braun, J. (2013): Climate change impacts on global food security. – *Science* 341: 508-513.
- [31] Wu, K. (2011): Influence of climate warming on the agriculture in Shenbei New District of Shenyang. – *Journal of Anhui Agri. Sci* 39(16): 9918-9920.
- [32] Xu, X. K., Wang, X. T., Jin, X. Q. (2009): Vegetation response to accumulated temperature patterns from 1960-2000 in China. – *Acta Ecologica Sinica* 29(11): 6042-6050.
- [33] Yan, M. H., Liu, X. T., Zhang, W., Li, X. J., Liu, S. (2011): Spatio-temporal changes of $\geq 10^{\circ}\text{C}$ accumulated temperature in Northeastern China since 1961. – *Chin. Geogra. Sci* 21(1): 17-26.
- [34] Yu, S., Yang, J., Liu, G., Yao, R., Wang, X. (2012): Multiple time scale characteristics of rainfall and its impact on soil salinization in the typical easily salinized area in Huang-Huai-Hai Plain, China. – *Stochastic Environmental Research and Risk Assessment* 26(7): 983-992.
- [35] Zhang, L., Li, M., Wu, Z., Liu, Y. (2011): Vegetation cover change and its mechanism in northeast China based on SPOT/NDVI data. – *Journal of Arid Land Resources and Environment* 25(1): 171-175 (in Chinese).
- [36] Zhao, W., Zhang, Y., Zhang, F., Wang, Q., Zhai, X., Qiu, N., Zhang, M. (2016): Influence of meteorological factors variation on yield components during maize grain-filling stage in East Gansu. – *Chinese Agricultural Science Bulletin* 32(21): 62-66.